45th AIAA/ASME/SAE/ASEE Joint Propulsion Conference & Exhibit
2 - 5 August 2009, Denver, Colorado

AIAA 2009-4913

Implementation of the kinetic Bohm condition in a Hall thruster hybrid code

Robert Santos* and Eduardo Ahedo†
Universidad Politécnica de Madrid, Madrid 28040, Spain

This work investigates the implementation of the accurate Bohm condition in a Hall Thruster hybrid code. First, an extended review of the current PIC weighting algorithms at boundaries is presented. Second, the accurate Bohm condition for non-monoenergetic, variable-charge populations is implemented. Third, a generalized PIC Mach-Bohm number is defined, based on the PIC weighting formulation of the kinetic Bohm condition. Fourth, the fulfilment of the accurate Bohm condition is analysed, showing that the best weighting scheme at boundaries lead to strong numerical oscillations. And finally, several advances in boundary weighting algorithms are presented aimed at reducing the oscillations of plasma magnitudes.

I. Introduction

In a Hall thruster the plasma is confined in a cylindrical annular chamber. A key factor to understand the discharge behavior of the plasma is the interaction with the walls, which strongly affects the efficiency and the lifetime of the thruster. This plasma-wall interaction has been a subject of research for a long time, from the early work of Tonks-Langmuir in 1929 to the present day. Tonks and Langmuir[14] showed that, in the zero Debye-lenghth limit, the plasma structure consists of thin non-neutral sheaths tied to the walls whith the Debye-length as the distinguished scale, and a quasineutral region (the *presheath*) occupying the bulk of the channel. Bohm showed that the formation of quasi-steady sheath solutions requires the fulfilment of one condition at the sheath entrance: the Bohm condition.[19]

The Bohm condition for a typical negative (i.e. ion-attracting) sheath can be interpreted as stating that the incoming ion flux is sonic or supersonic (for certain generalized sound speed). In its simple formulation for a plasma constituted by a cold ion-fluid, the Bohm condition is

$$M \equiv \frac{u_{ni}}{\sqrt{Z_i T_e / m_i}} \geq 1, \tag{1}$$

where T_e is the electron temperature, M stands for the ion-fluid Mach number (perpendicular to the wall), and u_{ni} is the ion-fluid velocity perpendicular to the wall (throughout the paper subindex n refers to the wall-perpendicular direction). More accurate expressions of the Bohm condition take into account the ion velocity distribution function, the presence of multiple ion species (with possitive and negative charge), and secondary electron emission from the dielectric walls.

In hybrid (PIC/fluid) quasineutral codes, the Bohm condition is of great relevance because is the condition to be imposed on the boundaries of the computational domain, which are the edges of

*PhD Candidate, robert.santos@upm.es, Full address: E.T.S. Ingenieros Aeronáuticos, Plaza Cardenal Cisneros, Madrid 28040, Spain, Student AIAA Member
†Professor, eduardo.ahedo@upm.es, Senior AIAA Member.

the Debye sheaths. The Bohm condition is also needed to compute correctly the electric potential profile in the presheath region.

Our quasineutral hybrid code is an updated version of the HPHall code originally developed by Fife and Martínez-Sánchez.[1,2] It is a time-dependent, axisymmetric code that simulates the plasma discharge in a Hall thruster chamber and near-plume, and consists of an anisotropic fluid subcode for the electrons[6] and a particle-in-cell (PIC) subcode for the heavy species. The two subcodes are advanced sequentially in time with a timestep Δt, and in each temporal advancement, the two subcodes interchange data in a feedback process: the electric potential and electron temperature fields, $\phi(\mathbf{r})$ and $T_e(\mathbf{r})$, are outputs of the electron subcode and inputs of the PIC subcode; reciprocally, particle densities and fluxes of neutrals (n) and ions (i), n_α, $\mathbf{g}_\alpha \equiv n_\alpha u_\alpha$, $(\alpha = n, i)$, are outputs of the PIC subcode and inputs of the electron subcode.

In this paper we discuss two issues. The first one is that a more accurate formulation of the Bohm condition must be used, rather than the simple expression (1), because the actual ion population in a Hall thruster is constituted of both singly-charged and doubly-charged particles and a widespread velocity distribution. The second one is how to implement that Bohm condition in a hybrid code, since there is not an immediate way of imposing the Bohm condition for a PIC formulation of the ions, and related work[9,10] has shown that the Bohm condition is not fulfilled naturally in PIC simulations. Alternative weighting algorithms at the boundaries nodes[11] have been proposed to solve that question, but most of them suffer from (or lead to) strong numerical oscillations of plasma magnitudes at boundaries. We report several advances in boundary weighting algorithms to (i) improve the fulfilment of the Bohm condition, and (ii) to reduce the numerical noise at boundaries.

The rest of the paper is organized as follows. Section 2 reviews the weighting algorithms at the boundaries implemented in the different versions of HPHall. Section 3 shows the accurate formulation of the Bohm condition in a particle-in-cell code. Section 4 discusses the proposed new boundary weighting algorithm.

II. Review of weighting algorithms

A. About the PIC code

The PIC code[21] is a kinetic method widely used to simulate plasmas. In this method the plasma is simulated as a collection of test particles, where each test particle represents a huge number of ions, neutrals or electrons. The test particles are moved under the action of an electromagnetic field, which is updated every timestep, and a Montecarlo's algorithm (MMC) is used to simulate the collisional processes (ionization, injection, recombination). A mesh is used for the spatial discretization of the physical domain. The cell typical length, ΔL, of the *standard mesh* (fig. 1(a)) is smaller than the expected gradient length of plasma inhomogeneities, but large enough to reduce the computational cost of the whole code. The electrommagnetic field is computed in the mesh nodes, and then interpolated to particle positions (gathering process) to push the particles. Reciprocally, the particle currents are deposited from particle positions to the mesh nodes (scattering process).

The particles have a spatial distribution or *shape functions* to avoid too much noise in the plasma magnitudes. The location and velocity of the particles correspond in fact to the center of mass of their spatial distribution, and is assumed that particles are non-deformable, that is, the whole particle moves with the same velocity. The summation of all test particles shows an approximate velocity distribution function of each species of the plasma.

An important issue in the PIC method is the *weighting* process, which computes the macroscopic magnitudes of heavy species at the nodes of the simulation mesh. This process is the PIC-equivalent

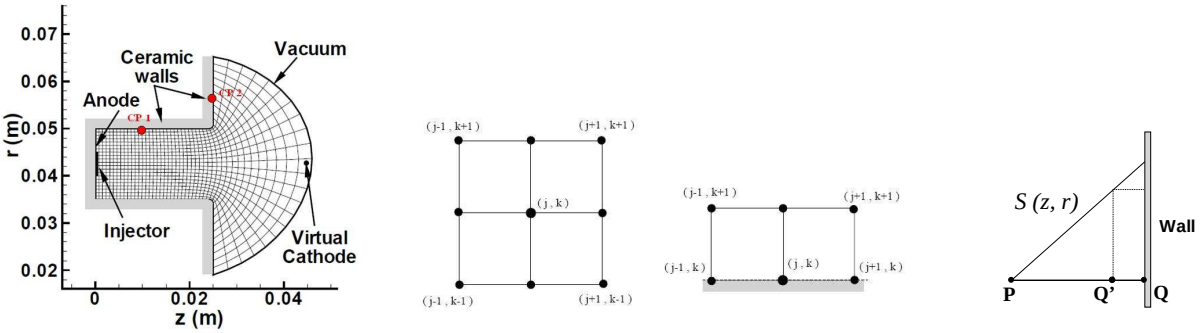

(a) (b) (c)

Figure 1. (a) Sketch of a typical simulation domain of HPHall. Two boundary test nodes are red-marked at locations (in cm) $CP1 \equiv (1.25, 5.00)$, and $CP2 \equiv (2.50, 5.65)$, respectively. (b) Sketch of the influence region of different nodes for the volumetric (first-order) weighting. (c) The asymmetric volumetric (first-order) weighting at the boundary nodes. Weighted plasma magnitudes are representative of the 'center of mass' Q'.

to take moments of the distribution function, that yield the density, the flux, the temperature, etc. of each species of the plasma. Essentially the weighting process is an average of the near particle properties within a control region of the computational domain.

B. Volumetric Weighting (VW) at internal nodes

This is the standard weighting scheme at the internal nodes of a PIC code. In this scheme, a volume of influence around an interior grid node is defined, and the properties of the particles within that volume are averaged. The average computation is done using a weighting function, which is defined in the volume of influence. This weighting function is identical to the shape function of the particles, and its role is capital to connect the 'particle' and 'node' points of view of the PIC codes.

The volumetric weighting of a property χ of species j at a generic node is

$$\langle \chi \rangle_{VW} = \frac{1}{\Delta V} \sum_p S(z_p, r_p) \frac{M_p}{m_i} \chi_p \tag{2}$$

where the sumation is extended to all particles of species j, χ_p is the particle property corresponding to macroscopic property χ, M_p/m_i is the number of atoms in the test particle (M_p is the mass of the particle and m_i is the atomic mass), $S(z_p, r_p)$ is the weight function (and particle shape function), and ΔV is the volume of influence of the node, weighted with the weight function in order to take cylindrical effects into account.[20]

Ion density, ion density current, and ion energy density are defined as $\langle 1 \rangle_{VW}$, $\langle eZ\mathbf{v} \rangle_{VW}$, and $\langle m_i v^2/2 \rangle_{VW}$, respectively, where Z is the charge number and $\mathbf{v}$ is the particle velocity.

Generally, the best trade-off between accuracy and computational cost is the shape function of order one. That bilinear function decreases linearly from 1 at the node location to zero at the sides of the parallelogram formed by the four neighboring nodes, Fig. 1(b). A higher-order shape function leads to more accurate computations and less noisy results, but increases considerably the computational effort. The refinement of the mesh is the alternative way of increasing the accuracy.

Although the volumetric weighting scheme is very useful in internal nodes of the computational grid, is not well suited for boundary nodes, just where the Bohm condition must be satisfied. In the original HPHall, Fife[2] used the VW at the boundary nodes limiting the volume of influence to the half-internal side, Fig. 1(b). This asymmetric weighting at the boundary nodes understimates

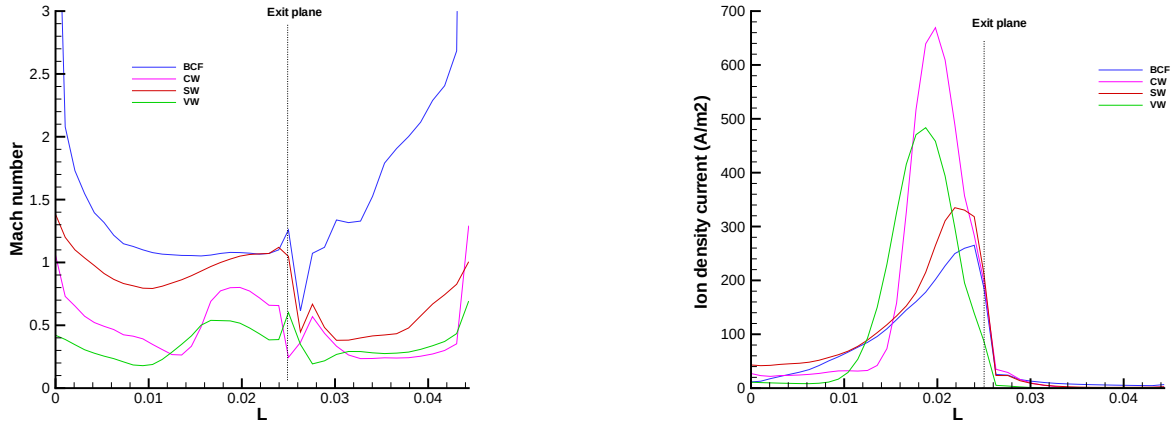

(a) (b)

Figure 2. Comparison of the four weighting algorithms at the nodes of the outer wall for a standard simulation mesh. (a) Mach number and (b) ion density current (A/m^2).

[overstimates, resp.] magnitudes that increase [decrease, resp.] toward the boundary. The error, proportional to ΔL_n (i.e. the cell length in the wall perpendicular direction), is large for magnitudes that present large gradients near the sheath boundary, which is the case of n_e and ϕ (but not g_{ni}).

C. Corrected Volumetric Wighting (CW)

Parra and Ahedo[10] observed that the application of Eq.(2) to the boundary-node half-volume of influence yields plasma magnitudes representative of the 'center of mass' Q' of that volume instead of the boundary node. For a linear weight-function, that center of mass is located at $\mathbf{x}_{Q'} = (2\mathbf{x}_Q + \mathbf{x}_P)/3$, Fig. 1(b). Then, they concluded that the correct volumetric weighting at a boundary node is an extrapolation of the weightings at points Q' and P

$$\langle\chi\rangle_{CW,Q} = \frac{3}{2}\langle\chi\rangle_{VW,Q'} - \frac{1}{2}\langle\chi\rangle_{VW,P}\,. \tag{3}$$

The application of this corrected volumetric weighting makes the error proportional to ΔL_n^2 and means a clear increase in the Mach-Bohm number and the wall plasma flux, with respect to the VW, Fig. 2, but the CW is still far from reaching a sonic Mach-Bohm number for a standard mesh. Besides, an occasional error of this extrapolating algorithm is to yield too low values of the plasma density.

There are more possible extrapolation schemes to obtain accurate computations of the plasma magnitudes at boundary nodes. One possibility is to use the information of more nodes, in a similar way as is done in the finite difference method. Another possibility consists of defining higher order extrapolation functions that may include in some manner the asymptotic transition to the sheath. But, although these methods seem to be promising, some numerical experiments suggested other simpler ways to improve the results.

D. Bohm Condition forcing (BF)

As an alternative to the corrected volumetric weighting, Parra and Ahedo[10] proposed an algorithm that forces the fulfilment of the Bohm condition. The algorithm, to be applied to the plasma

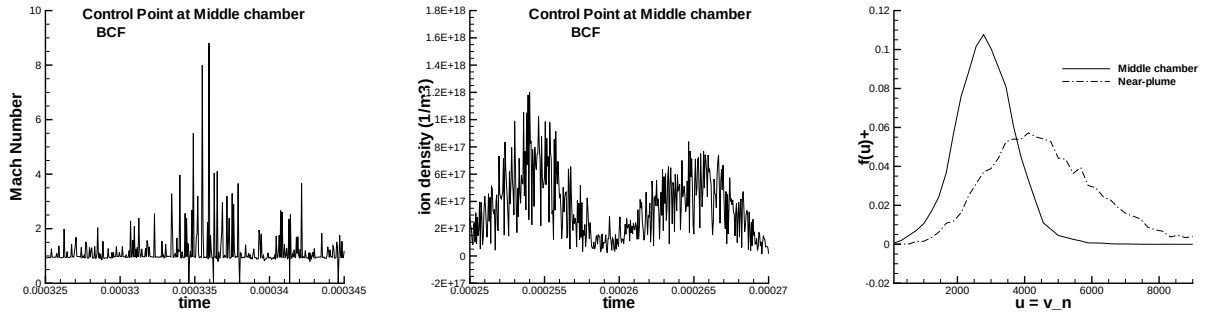

(a) (b) (c)

Figure 3. Bohm condition forcing. Temporal oscilations (in $\backsim 10\mu s$) of the (a) Mach number, and (b) ion density ($1/m^3$) at test points of the outer wall of the thruster. (c) Single-ion distribution function at test points.

density, is

$$n_e|_{BF} = min\left\{\frac{g_{ni}|_W}{\sqrt{ZT_e/m_i}}, n_e|_W\right\}; \tag{4}$$

where W means the selected weighting algorithm (VW, CW or the surface weighting algorithm explained below). This algorithm is based on forcing the ion flux to satisfy the (simple form of the) Bohm condition whenever the weighting scheme is not able to achieve it. This is performed in three steps: (i) assuming that the ion macroscopic velocity normal to the walls is the Bohm velocity, (ii) considering that the weighting scheme yields the correct ion flux at the boundary, and (iii) correcting the density at the boundary nodes in order to match the computed ion flux. Since this is just a local adjustment, the ion flux g_{ni} is not affected by it. The other plasma magnitudes are computed in a similar manner using the corrected values of the density and velocity.

Although the BF algorithm represents an intrusive algorithm likewise artificial to the PIC code, it yields, for a standard mesh, excellent results in terms of plasmas fluxes and the development of the plasma structure perpendicular to the wall. But the experience shows that the BF can produce very large oscillations of the plasma magnitudes at the boundary nodes, as Fig. 3(a) and 3(b) illustrates. The explanation would be that forcing the Bohm condition leads to an overexcitation in the coupling of the plasma density and the electric potential. These perturbations not only affect the sheath solutions, but also the presheath solution since the perturbations may travel along the magnetic lines as ion-acoustic waves.

In an attempt to mitigate the oscillations on the Mach number and to adapt the BF to simulations with single and double ions, Hofer et al., working with HPHall-2,[3] modify the algorithm Eq.(4) and introduce a couple of tuning parameters that adjust to their satisfaction.

In a likewise context, Hutchinson[22] argued that the Bohm condition cannot be applied at each timestep because the inherent particle fluctuations, and presented a feedback algorithm to adjust smoothly the potential over several timesteps.

Another objection to the BF algorithm is that Eq.(4) it is not applicable for the kinetic formulation of the Bohm condition, since it is valid only for a cold, single-charged ion population. Figure 3(c) shows the dispersion in the particle distribution function for singly-charged ions.

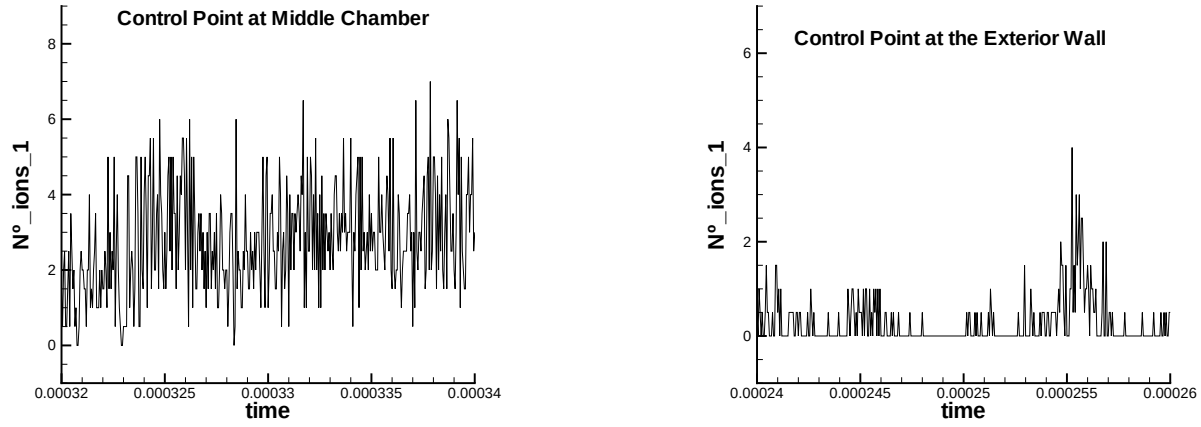

(a) (b)

Figure 4. Surface Weighting. Temporal oscillations (in $\backsim 10\mu s$) of the number of ions crossing the boundary during each timestep at test points located at the outer wall of the thruster: (a) the middle chamber, and (b) the exterior front wall.

E. Surface Weighting (SW)

This algorithm was proposed by Parra[13] and is based on measuring surface properties instead of volume properties. The SW algorithm is

$$\langle \chi \rangle_{SW} = \frac{1}{\Delta A \Delta t} \sum_p S(z_p, r_p) \frac{M_p}{m_i} \frac{\chi_p}{v_{np}} \tag{5}$$

where the summation index applies to all particles that cross the boundary node area-of-influence, ΔA, during the time interval Δt, and $S(z_p, r_p)$ is the weight-function defined in this area. A zeroth order weight-function is used because higher orders need the impact coordinates of every particle crossing the surface.

Ion density, ion density current, and ion energy density are defined as $\langle 1 \rangle_{SW}$, $\langle eZ\mathbf{v} \rangle_{SW}$, and $\langle m_i v^2/2 \rangle_{SW}$, respectively. Nonetheless, observe that the basic magnitudes of the VW and the SW are the particle density, $\langle 1 \rangle_{VW}$, and the particle flux, $\langle v_n \rangle_{VW}$, respectively.

For a standard mesh, the SW yields acceptable values of the Mach number, larger than those of the CW and a bit smaller than those of the BF, Fig. 2. The error associated to the SW algorithm is only ΔL_n^2 (due to the discretization of the electric potential, mainly), and the obtained value $\langle \chi \rangle_{SW}$ represents a time average in Δt of χ.

The SW produces smaller oscillations of the Mach number than the BF, but the current implementation of the SW is very noisy numerically because the number of particles considered in each timestep Δt is small and presents a large dispersion, as Fig. 4 illustrates.

III. The PIC Bohm condition

The electrostatic potential in a thin, collisionless sheath satisfies the Poisson's equation

$$\frac{d^2\phi}{dz^2} = -\frac{e}{\epsilon_0} \sum_j Z_j n_j(\phi), \tag{6}$$

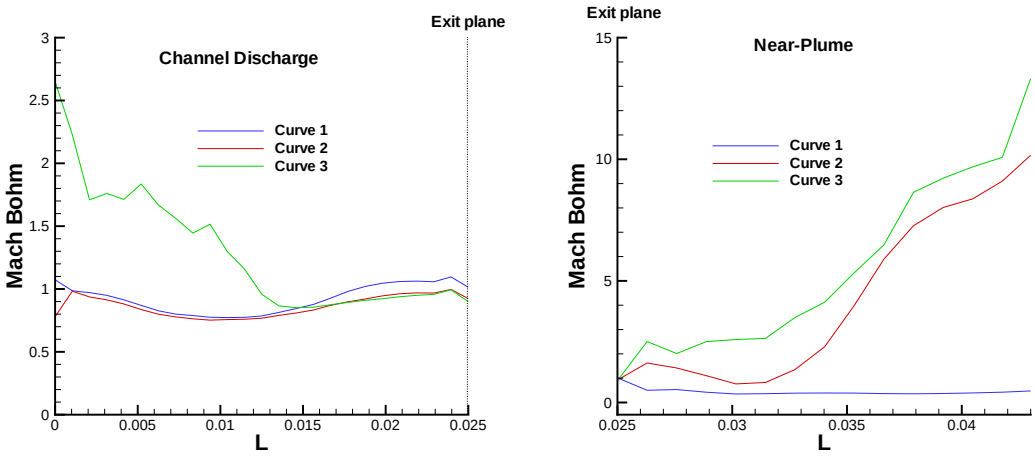

(a) (b)

Figure 5. Comparison of Mach-Bohm numbers at the outer wall of the thruster in (a) the channel discharge and (b) the near-plume region, using the SW algorithm. Curve 1 is the simple Mach number, Eq. (1), for a simulation with singly-charged ions only. Curve 2 is the PIC Mach-Bohm number for the same simulation than curve 1. Curve 3 is the PIC Mach-Bohm number for the same simulation but including doubly charged ions.

where subindex j stands for the different species of a multicomponent plasma (with possitive and negative charge), and Z_j for its charge number. The Bohm condition at the sheath edge Q is

$$\sum_j Z_j \left.\frac{dn_j}{d\phi}\right|_{Q+} \leq 0 \tag{7}$$

and stems from imposing that the non-neutral solution of Poisson's equation that starts from Q corresponds to a locally monotonic potential (i.e. it dismisses oscillatory solutions).

For a negative (i.e. ion attracting) sheath, and a single electron population close to a Maxwell-Boltzmann equilibrium inside the sheath, the Bohm condition at Q becomes

$$0 \leq S \equiv \frac{\alpha_e}{T_e}\sum_i Z_i n_i - \sum_i \frac{Z_i}{e}\frac{dn_i}{d\phi}, \tag{8}$$

where: summation index i stands now only for ion species, $\alpha_e - 1$ accounts for deviations from the Maxwell-Boltzmann equilibrium (like a partially depleted Maxwellian), and plasma quasineutrality at the sheath edge, $n_e = \sum_i Z_i n_i$, was invoked. Then, $n_i(\phi)$ and the Bohm function S depend on the formulation chosen for the ions. In a Hall thruster, the kinetic formulation for the ions represents the most suitable choice, and leads to

$$S = \frac{\alpha_e}{T_e}\langle Z\rangle - \left\langle \frac{Z^2}{m_i v_n^2}\right\rangle, \tag{9}$$

$$\langle\chi\rangle = \sum_i \int_0^\infty dv_n f_{iQ}(v_n)\chi_i(v_n), \tag{10}$$

where the summation index i extends to the several ion populations (of different charge numbers, for instance) v_n is the particle velocity perpendicular to sheath and wall, and f_{iQ} is the ion velocity distribution function after taking moments over the two other velocity components.

The PIC formulation of the Bohm condition is obtained using the selected weighting scheme for the computation of $\langle\chi\rangle$ at the boundary nodes. Thus for the SW one has

$$S = \frac{1}{\Delta t \Delta A} \sum_p \frac{Z_p}{v_{np}} \frac{M_p}{m_i} \left(\frac{\alpha_e}{T_e} - \frac{Z_p}{m_i v_{np}^2} \right). \tag{11}$$

Notice that the simple Bohm condition (1) is recovered by the kinetic formulation if $f_{iQ}(v_n)$ is a Dirac function, and by the PIC+SW formulation if all particles have the same velocity $v_{np} = u_{ni}$.

A convenient parameter for evaluating how close the plasma behavior is to the 'sonic' Bohm condition $S = 0$ is the generalized Mach-Bohm number

$$M = \sqrt{\frac{m_i \alpha_e}{T_e} \frac{\langle Z \rangle}{\langle Z^2 v_n^{-2} \rangle}} \tag{12}$$

that transforms $S \geq 0$ into $M \geq 1$. Notice that the velocity involved in this definition is not the average ion velocity, $\langle v_n \rangle$, but $\langle Z \rangle^{\frac{1}{2}} \left\langle Z^2 v_n^{-2} \right\rangle^{-\frac{1}{2}}$. Particles or ions with low velocities (presumably created near the boundary) tend to decrease M and make more difficult the fulfilment of $S \geq 0$. This is not a defect of the definition, but the evidence of the physical fact that low-velocity particles are more affected by decrements of ϕ and therefore contribute more to increase $dn_i/d\phi$ at the sheath edge.

Figure 5 shows the difference between the simple Mach-Bohm number, eq. (1), and the generalized PIC Mach-Bohm number, eq. (12). In the performed simulations, the SW algorithm was used to weight at boundaries, and two cases were studied: (1) singly-charged ion population and (2) singly and doubly-charged ion populations. The large oscillations of the electric field at the exterior front wall of the thruster would be the reason to achieve the observed high value of the Mach-Bohm number.

IV. Improved weighting at the boundaries

A. Extended surface weighting (ESW)

The main cause for the numerical noise created by surface weighting is the number of particles crossing a boundary node panel in the time Δt, which oscillates much and has a small mean value. The PIC timestep is upper bounded by $\Delta t \backsim$(typical-cell-half-length)/(typical-particle-velocity), with the aim of limiting the statistical noise of the volumetric weighting. But it is immediate that the reduction of statistical noise of the SW requires a higher timestep for its measurement, such that enough particles cross the node panel. A simple estimate gives that the minimum timestep for the zeroth order SW should be about one-order-of-magnitude larger than Δt for having a similar level of noise than the first-order VW at internal points.

This suggests that the SW algorithm should sum particles crossing the boundary over several (say k) PIC timesteps, that is during the time interval $k\Delta t$. Thus, an extended or dynamic-mean surface-weighting algorithm is

$$\langle\chi\rangle_{SW(D)} = \frac{1}{k \Delta t \Delta A} \sum_k \sum_p \frac{M_p}{m_i} \frac{\chi_p}{v_{np}}, \tag{13}$$

where the summation on k is extended to the last k-timesteps. This algorithm decreases the numerical noise as k^{-1}, as Fig. 6(b) illustrates. The requirement of memory increases with k but this is not a severe limitation, since only the boundary nodes are involved. The upper-bound of k depends on two other criteria. The first one is the level of numerical noise of the rest of the code

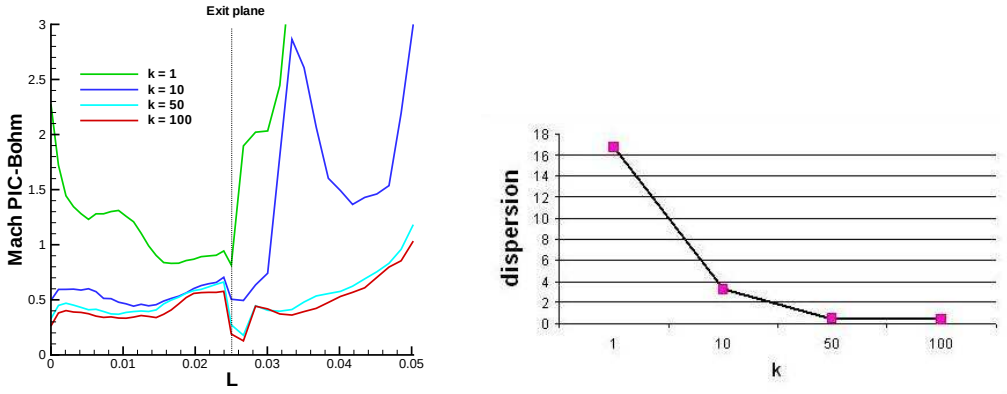

(a) (b)

Figure 6. Extended Surface Weighting. (a) Evolution of the mean Mach-Bohm number with k, the number of timesteps, along the outer wall of the thruster. (b) Dispersion (standard deviation) of the Mach-Bohm number with respect to k at a test point of the outer wall.

algorithms. The second and possibly more important one is the frequency of physical oscillations that we want the full code be able to simulate. A reasonable upper-bound for physical oscillations with this code would be of 1 Mhz or less. Then, for $\Delta t = 10^{-8}$, the upper-bound of k would be $\backsim 20 - 50$.

Figure 6(a) shows, along the outer wall of the thruster, the mean Mach-Bohm number (12) using the ESW algorithm for different time intervals $k\Delta t$. For $k = 1$, which is equivalent to use the original SW algorithm, the Mach-Bohm number is very satisfactory in the channel discharge ($M \backsim 1$), but surprisingly high in the near-plume region ($M \backsim 10$). The case $k = 10$ represents a great reduction of the Mach-Bohm number in the low-density regions of the thruster, such as the near-plume region and the near-anode region, but in the channel discharge the Mach-Bohm number is half-reduced. And cases $k = 50$, and $k = 100$, reinforce the idea that a higher value of k makes more homogeneous the Mach-Bohm number along the thruster, but reducing it to a value $M \backsim 0.4$, in a somehow asymptotic behavior.

The high value of the Mach-Bohm number using the ESW with k below 10 is due to the large temporal oscillations showed in fig. 7. The mean value of the Mach-Bohm number is increased by the high picks achieved at some instants in the Mach-Bohm number evolution. The same large oscillations are obtained in the evolution of the plasma density and the electric potential at the boundary nodes, but not for the electron temperature, which is not much affected. Figure 8 shows the reduction of these oscillations using fifty PIC-timesteps in the weighting computations at boundaries. The measured oscillations of the plasma magnitudes have a frequency of $\backsim 100Khz$, and they seem to be of physical type.

B. Generalized Bohm forcing and PIC Mach-Bohm forcing

The difficulties of the weighting algorithms to fulfill the Bohm condition suggest the study of other numerical methods. Since the particles are accelerated by the electric field, corrections of the electric potential at the boundary nodes will improve the fulfillment of the Bohm condition. Following this idea, two kind of methods are presented. The first one is the *Generalized Bohm forcing*, and is based on a node potential adjustment $\delta\phi$ to make $S = 0$. This potential adjustment changes the velocity of a particle crossing the boundary from v_{np} to v'_{np}, conserving its total energy, that is $m_i v'^2_{np} = m_i v^2_{np} + 2e\delta\phi$. Then, applying $S = 0$ and the ESW scheme, $\delta\phi > 0$ is obtained from the

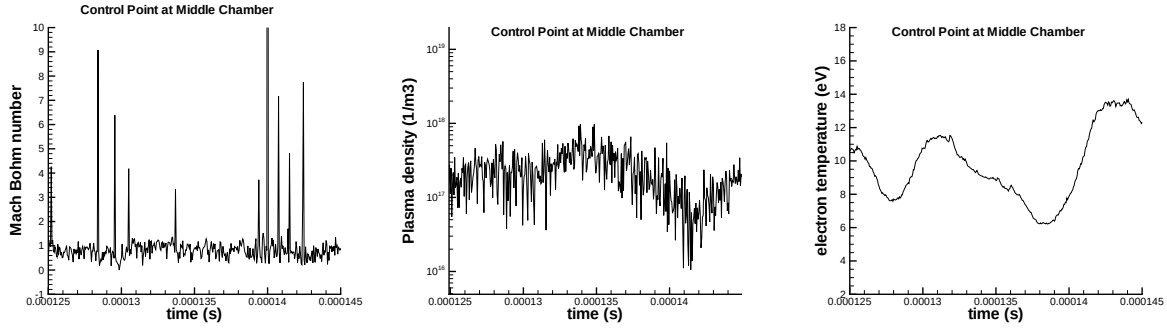

(a) (b) (c)

Figure 7. Extended Surface Weighting with $k = 1$. Temporal oscillations (in $\backsim 10\mu s$) of (a) the PIC Mach-Bohm number (12), (b) the plasma density, and (c) the electron temperature, at a test point of the outer wall of the Hall thruster chamber.

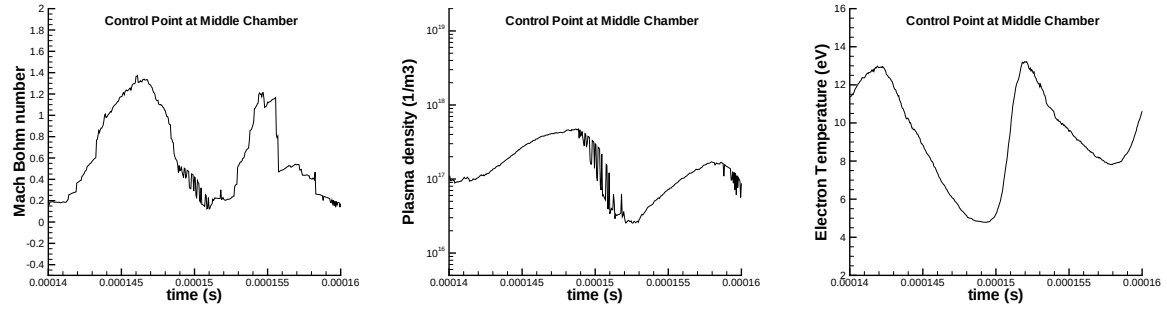

(a) (b) (c)

Figure 8. Extended Surface Weighting with $k = 50$. Reduction of the temporal oscillations (in $\backsim 10\mu s$) of (a) the PIC Mach-Bohm number (12), (b) the plasma density, and (c) the electron temperature, at a test point of the outer wall of the Hall thruster chamber.

implicit equation

$$\sum_k \sum_p \frac{Z_p}{v'_{np}} \frac{M_p}{m_i} \left(\frac{\alpha_e}{T_e} - \frac{Z_p}{m_i v'^2_{np}} \right) = 0 \tag{14}$$

The solution of eq. (14) leads to a sub-iterative process in each PIC timestep, where the ion particles crossing the boundary must be updated in each sub-iteration. Other simpler ways to solve eq. (14) involves the variation of the function S with respect to the electric potential. But these possibilities are still a subject of research.

The second method to correct the electric potential at boundary nodes is the *Mach-PIC forcing*, and is based on a potential adjustment obtained from the equation

$$\delta\phi = \frac{T_e}{e} \ln\left(M^\gamma\right) \tag{15}$$

where T_e is the electron temperature in eV, M is the PIC Mach-Bohm number (12), and γ is a parameter tuned for convenience.

This method is purely of numerical type, not based on physical arguments, but is easier to implement than the Generalized Bohm forcing. The first numerical experiments have shown an appreciable improvement of the Bohm condition, but further studies must be made in order to validate the method.

Acknowledgments

This research was financed by the Ministerio de Educación y Ciencia of Spain, under project ESP-2007-62694.

References

[1]J. Fife and M. Martínez-Sánchez, Comparison of results from a two-dimensional numerical SPT model with experiment, in *32nd Joint Propulsion Conference, Lak Buena Vista, FL*, AIAA-1996-3197, American Institute of Aeronautics and Astronautics, Washington, DC, 1996.

[2]J. M. Fife, *Hybrid-PIC Modeling and Electrostatic Probe Survey of Hall Thrusters*, PhD thesis, Massachusetts Institue of Technology, 1998.

[3]F. Parra, E. Ahedo, M. Fife, and M. Martínez-Sánchez. Journal of Applied Physics **100**, 023304 (2006).

[4]F. Parra, D. Escobar, and E. Ahedo, Improvements on particle accuracy in a Hall thruster hybrid code, in *42th Joint Propulsion Conference, Sacramento, CA*, AIAA-2006-4830, American Institute of Aeronautics and Astronautics, Washington, DC, 2006.

[5]I. Maqueda, D. Escobar, and E. Ahedo, Advances on a Hall thruster hybrid code, in *30th International Electric Propulsion Conference, Florence, Italy*, IEPC 2007-066, Electric Rocket Propulsion Society, Fairview Park, OH, 2007.

[6]D. Escobar and E. Ahedo, IEEE Transactions on Plasma Science **36**, 2043 (2008).

[7]D. Escobar, A. Antón, and E. Ahedo, Simulation of high-specific-impulse and double-stage Hall thrusters, in *Proc. 29th International Electric Propulsion Conference, Princeton, USA*, IEPC-2005-040, Electric Rocket Propulsion Society, Fairview Park, OH, 2005.

[8]S. Barral and E. Ahedo, Physical Review E **79**, 046401(1) (2009)

[9]F. Parra, E. Ahedo, M. Martínez-Sánchez, and J. Fife, Improvements of the plasma-wall model on a fluid-PIC code of a Hall thruster, in *SP-555: 4th Spacecraft Propulsion Conference, Sardinia (Italy)*, European Space Agency, Noordwijk, The Netherlands, 2004.

[10]F. Parra and E. Ahedo, Fulfillment of the Bohm condition on the HPHall fluid-PIC code, in *Proc. 40th Joint Propulsion Conference, Fort Lauderdale, FL*, AIAA 2004-3955, American Institute of Aeronautics and Astronautics, Washington, DC, 2004.

[11]D. Escobar, E. Ahedo, and F. I. Parra, On conditions at the sheath boundaries of a quasineutral code for Hall thrusters, in *Proc. 29th International Electric Propulsion Conference, Princeton, USA*, IEPC-2005-041, Electric Propulsion Society, Fairview Park, OH, 2005.

[12]A. Antón, D. Escobar, and E. Ahedo, Contour algorithms for a Hall thruster hybrid code, in *42th Joint Propulsion Conference, Sacramento, CA*, AIAA-2006-4834, American Institute of Aeronautics and Astronautics, Washington, DC, 2006.

[13]F. Parra, Actualización y mejora de un código pic-fluido bidimensional para el flujo de plasma en motores de efecto Hall, Master's thesis, Escuela Técnica Superior de Ingenieros Aeronáuticos, Universidad Politécnica de Madrid, 2004.

[14]E. Harrison and W. Thompson, Proc. Physical Society of London **74**, 145 (1959).

[15]K. Riemann, IEEE Transactions On Plasma Science, **23**, 709 (1995).

[16]K. Riemann, J. Phys. D: Appl. Phys., **24** 493-518 (1991).

[17]E. Ahedo, Physics of Plasmas **9**, 4340 (2002).

[18]E. Ahedo and D. Escobar, Physics of Plasmas **15**, 033504 (2008).

[19]D. Bohm, Minimum ionic kinetic energy for a stable sheath, in *The characteristics of the electrical discharge in magnetic fields*, A. Guthry and W.K. Wakerling. Eds. New York: McGraw-Hill, 1949, ch. 3, p. 77.

[20]J. P. Verboncoeur, *Symmetric Spline Weighting for Charge and Current Density in Particle Simulation*, Journal of Computational Physics 174, 421 (2001).

[21]C. K. Birdsall and A. B. Langdon. *Plasma Physics via Computer Simulation*. IOP Publishing Ltd. (1991).

[22]I. H. Hutchinson, Plasma Phys. Control. Fusion **44**, 1953-1977, (2002).